J. Fluid Mech. (1969), *vol.* 36, *part* 1, *pp.* 127–143
Printed in Great Britain

The two-dimensional flow of a stratified fluid over an obstacle

By RUSS E. DAVIS

Institute of Geophysics and Planetary Physics,
University of California, La Jolla

(Received 19 June 1968)

The two-dimensional stratified flow over an obstacle placed in a channel of finite height is examined to determine the extent to which Long's model provides an adequate description of real flows. A simple numerical method of solving Long's model for obstacles of arbitrary shape is used to calculate predicted streamline patterns which are compared with experimental observations of the flow over two bluff obstacles. If only a few lee-wave modes are excited there is qualitative agreement between theory and experiment, but, if the flow is subcritical with respect to several lee-wave modes, the effects of turbulence become dominant and the inviscid model is no longer useful. The theory predicts that the drag on an obstacle can increase with decreasing speed owing to the momentum transfer to lee-wave motion. Direct measurement of drag indicates that there are conditions under which the drag does increase with decreasing speed, but under these conditions the wake is dominated by turbulence and no lee waves can be detected.

Introduction

For a number of years the study of stratified flow over obstacles was limited to mathematical analyses based on the linearization of Euler equations and the appropriate boundary conditions. But in 1953 Long showed that, for the special case of constant dynamic pressure and uniform vertical density gradient far upstream of the obstacle, the full equations of steady, two-dimensional inviscid flow could be transformed to a linear one, namely Helmholtz's equation. This equation, coupled with the appropriate boundary conditions on the bounding surfaces and the assumption that there are no waves far upstream, represents a well-posed linear boundary-value problem which has served as the basis of several analyses of flow over obstacles of finite size. Owing to the difficulties presented by the boundary conditions on the obstacle, the earlier analyses of Long (1955) and Yih (1960) made use of an inverse method in which the exact shape of the object is determined only after the solution is complete and it was not until Drazin & Moore (1967) constructed solutions for flow over a thin vertical strip that a detailed description of the flow over a prescribed obstacle for a wide range of stratifications became available.

The work of Drazin & Moore disclosed the puzzling prediction that, for a given stratification, the drag on a barrier of fixed height apparently increases without

bound as the flow velocity decreases. This effect is presumably a manifestation of the fact that as the upstream velocity is reduced the flow becomes subcritical with respect to an increasing number of lee-wave modes, each of which contributes to the wave drag. Only recently Miles (1968*a*, *b*) has investigated the wave drag associated with stratified flow past various obstacles using approximation techniques which avoid the extensive algebraic computations employed by Drazin & Moore. In addition to providing more complete information about the thin barrier in a finite channel, Miles presented drag predictions for both a thin barrier and a semicircular obstacle in an unbounded fluid. In all of these cases it was again found that as the free-stream velocity is reduced the drag on the obstacle is increased. However, as Miles pointed out, this surprising proposition is subject to the requirement that Long's model is an adequate description of real flows and there are several reasons, such as the existence of significant viscous effects or upstream waves, why this may not be the case. Perhaps an even more serious objection is that the solutions obtained from Long's model often indicate both regions of closed streamline flow, which are inconsistent with the model itself, and regions in which the density increases with height, a configuration which is likely to be unstable.

Unfortunately, the extensive theoretical investigation of stratified flow over obstacles has not been paralleled by experimental work and to date Long's (1955) experiments are the only ones with which the theories may be compared. Consequently, it is the purpose of the present study to supplement these experiments and in particular to attempt to answer the questions concerning the validity of the basic theoretical model which have been raised by the recent work of Miles (1968). In what follows we shall consider again the problem first posed by Long and, using a simple numerical method, obtain solutions corresponding to flow over obstacles of arbitrary shape placed in a channel of finite depth. These solutions will then be compared with experimental observations of the flow around obstacles towed through a tank filled with a stratified salt water solution. It will be shown that the discrepancy between theory and experiment, which is often very great, is associated with the generation of intense turbulence behind the obstacle. The structure of the turbulent wake is strongly influenced by the stratification and, in fact, bears little resemblance to the wake behind bluff bodies in unstratified flow. Results of the direct measurement of both total drag and wave drag show that this turbulent wake plays a dominant role in the flow.

Theoretical model

Following the notation of Miles (1968*a*) in which all lengths are made dimensionless using the characteristic length H/π, where H is the channel depth, Long's model is obtained if

$$\rho(y)U^2(y) = q \tag{1a}$$

and

$$-g\frac{d\rho}{dy}\frac{H}{\pi}\Big/q = k^2, \tag{1b}$$

where $\rho(y)$ and $U(y)$ are the density and horizontal velocity far upstream of the

obstacle, y is the dimensionless elevation and q and k^2 are constants. The equation of motion then becomes (see Long 1955)

$$\nabla^2\delta + k^2\delta = 0, \tag{2}$$

where δ is the dimensionless vertical displacement of a streamline from its elevation far upstream. Kinematic conditions on each of the surfaces which bound the fluid yield the boundary conditions

$$\delta + y = C_i \tag{3a}$$

on each surface S_i and the requirement of no upstream waves, that is

$$\delta \to 0 \quad \text{as} \quad x \to -\infty, \tag{3b}$$

completes the specification of the problem.

In the derivation of (2) it has been assumed that every streamline in the flow extends to the undisturbed region far upstream, an assumption which excludes the occurrence of regions of closed streamline flow. If the obstacle is external to the flow in the sense that it is a distortion of one of the bounding surfaces of the channel, then the constant in (3a) is easily determined; but, if the obstacle is internal to the flow, this constant, which specifies which streamline is in contact with the body, cannot be prescribed. This ambiguity, a familiar one in potential flow problems, can only be resolved by making some additional hypothesis concerning the nature of the flow. Because a sound basis for any such hypothesis is lacking, the theoretical development is limited to obstacles which comprise part of the boundary of the channel.

For obstacles of arbitrary shape the solution of the problem posed in (2) and (3) is most easily accomplished through the use of a Green's function. Thus, as Miles (1968a) has shown, the solution can be expressed in the form

$$\delta(x,y) = \int_{S'} \left\{\frac{\partial G}{\partial n}\delta(\xi,\eta) - G(\xi,\eta)\frac{\partial \delta}{\partial n}\right\} dl, \tag{4}$$

where S' is the surface of the obstacle and n is the outwardly directed normal to the surface. For values of k between the integers K and $K+1$ the appropriate Green's function satisfying (2) and (3b) is

$$G = -\frac{2}{\pi}H(x-\xi)\sum_{n=1}^{K}\alpha_n^{-1}\sin\alpha_n(x-\xi)\sin n\eta\sin ny$$

$$+\frac{1}{\pi}\sum_{K+1}^{\infty}\alpha_n^{-1}e^{-\alpha_n|x-\xi|}\sin n\eta\sin ny,$$

where H is the Heavyside step function and

$$\alpha_n = |k^2 - n^2|^{\frac{1}{2}}.$$

Using the boundary condition (3a) to determine δ on S', (4) becomes an integral equation for $\partial\delta/\partial n \equiv V$ on S'. Then, when V has been found, $\delta(x,y)$ can be computed directly from (4). While the solution of the integral equation is, in principle, straightforward, an explicit analytic solution can be found only for particular obstacle shapes and then only after some degree of approximation. Consequently,

recourse to a finite-difference technique appears to be necessary in order to obtain results for obstacles of arbitrary form.

The objective of the numerical scheme is to obtain a relatively small system of algebraic equations which is an accurate approximation of the integral equation (4). This is accomplished by first dividing the path along the obstacle surface into N segments of length ϵ_i which are centred at the points $\bar{x}_i, \bar{y}_i$ and have end-points x_i, y_i and x_{i+1}, y_{i+1}. Then in each interval both δ and V are expanded in Taylor series about the points $\bar{\xi}_i, \bar{\eta}_i$, leading to

$$\sum_i \left\{ \delta(\bar{\xi}_i, \bar{\eta}_i) \int_{\xi_i,\eta_i}^{\xi_{i+1},\eta_{i+1}} \frac{\partial G}{\partial n} dl - V(\bar{\xi}_i, \bar{\eta}_i) \int_{\xi_i,\eta_i}^{\xi_{i+1},\eta_{i+1}} G\, dl \right\} \simeq \delta, \tag{5}$$

where the error is dependent on the shape of the obstacle being $O(\epsilon)$ for a smooth body and $O(\epsilon^{\frac{1}{2}})$ for an object with a sharp corner at $l = l_0$ in the neighbourhood of which $V \sim (l-l_0)^{-\frac{1}{2}}$. In approximating the remaining integrals some care is required, since the Green's function has a logarithmic singularity at $x = \xi, y = \eta$. To overcome this difficulty, as well as to speed convergence of the series which must be summed, G is expressed as the sum of a singular part G_s and a regular part G_r, where

$$G_s = \frac{1}{\pi} \sum_{n=1}^{\infty} n^{-1} e^{-n|x-\xi|} \sin ny \sin n\eta = \frac{1}{4\pi} \ln \left(\frac{1 - 2e^{-|x-\xi|} \cos(y-\eta) + e^{-2|x-\xi|}}{1 - 2e^{-|x-\xi|} \cos(y+\eta) + e^{-2|x-\xi|}} \right)$$

and

$$G_r = \frac{1}{\pi} \sum_{n=1}^{K} \{ -2H(x-\xi) \alpha_n^{-1} \sin \alpha_n (x-\xi) - n^{-1} e^{-n|x-\xi|} \} \sin ny \sin n\eta$$

$$+ \frac{1}{\pi} \sum_{K+1}^{\infty} \{ \alpha_n^{-1} e^{-\alpha_n |x-\xi|} - n^{-1} e^{-n|x-\xi|} \} \sin ny \sin n\eta.$$

The accurate approximation of the integrals involved in (5) is then easily accomplished following the basic outline: (i) all integrals of G_r and $\partial G_r/\partial n$, as well as those integrals of G_s over paths which do not pass through the point (x, y), are computed as

$$\int_{\xi_i,\eta_i}^{\xi_{i+1},\eta_{i+1}} Q\, dl \simeq \epsilon_i Q(\bar{\xi}_i, \bar{\eta}_i);$$

(ii) the integral of G_s over a path passing very near (x, y) is obtained by noting that to $O[(x-\xi)^2 + (y-\eta)^2]$

$$\int G_s dl = \frac{1}{4\pi} \int \{ \ln[(x-\xi)^2 + (y-\eta)^2] - \ln[1 - 2e^{-|x-\xi|} \cos(y+\eta) - e^{-2|x-\xi|}] \} dl,$$

the second term of which may be obtained as in (i) while the first term is determined by approximating the integration path by several straight-line segments over which the integral is found analytically; (iii) because G_s is a harmonic function, it follows from Green's theorem that the integral

$$\int \frac{\partial G_s}{\partial n} dl$$

is independent of path and hence may be obtained by following lines parallel to the x- and y-axes along which the appropriate series are easily integrated term by term to yield forms for which the sum is known (see Jolley 1961).

Using the computational techniques outlined above, (5) is reduced to

$$\sum_{i=1}^{N} \delta(i)\, A(x, y; i) - V(i)\, B(x, y; i) = \delta(x, y), \tag{6}$$

where A and B are the appropriate approximations to the integrals of $\partial G/\partial n$ and G respectively. Substituting the known values of δ on the obstacle surface and requiring that (6) be satisfied at the N points $(\bar{\xi}_i, \bar{\eta}_i)$ yields a set of algebraic equations which can be solved for $V(\bar{\xi}_i, \bar{\eta}_i)$. These values, in turn, can be used to calculate δ throughout the entire flow field. The number of points was increased until V varied by less than 0·1 % when N was increased by 50 %; for the cases considered N was less than 50. Using this computational scheme an entire flow field can be computed on a Control Data Corporation 3600 in less than 1 min.

Before comparing the results of this numerical scheme with experimentally observed flows, it is of interest to consider the predicted amplitudes of the lee waves generated by an obstacle which has been treated by both Drazin & Moore (1967) and Miles (1968*a*), namely a vertical barrier of infinitesimal width. For this case the analysis is simplified, since the first term of the summation in (6) is identically zero. Taking this into account and noting the form of the Green's function, it can be seen that far downstream of the obstacle δ will approach the limit

$$\delta \sim -\sum_{n=1}^{K} \alpha_n^{-1} C_n \sin ny \sin \alpha_n x.$$

Hence, far downstream we find K lee-wave modes with amplitudes C_n/α_n and horizontal wave-number α_n.

Lee-wave amplitudes have been calculated both by Drazin & Moore and by Miles for the particular case of a barrier of dimensionless height $\frac{1}{4}\pi$ and their results are plotted in figure 1 along with the corresponding results obtained by the numerical method described above. In every case the agreement with the values reported by Drazin & Moore is nearly perfect. Similarly for the range $1 < k < 4$ the agreement with Miles's (1968*a*) variational approximation is quite good and it is not until k exceeds 4 that the approximate values become unreliable. Comparison of the tangential velocity $V(i)$ with the 'trial' function adopted by Miles indicates that this remarkable agreement is due, in large part, to the degree to which the 'trial' function approximates the true form.

Flow visualization experiments

The experiments discussed in this section were designed to determine the extent to which solutions of Long's model describe real stratified flows and the principal causes of any large discrepancies. The experiments reported by Long (1955) indicate that for small, streamlined obstacles there is a qualitative agreement between theory and experiment over a certain range of flow conditions but, as will be seen from the results to be presented, they do not adequately describe some of the important ways in which the theory breaks down. In fact it turns out that for reasonably large barriers the theory is adequate only over a small range of flow conditions.

The experiments to be described here were carried out in a Lucite tow-tank 2 m long, 18 cm deep and 18 cm wide which was filled with salt water. The salt concentration was adjusted to provide an approximately linear variation of density with depth. The total density difference typically ranged from 0·02 to

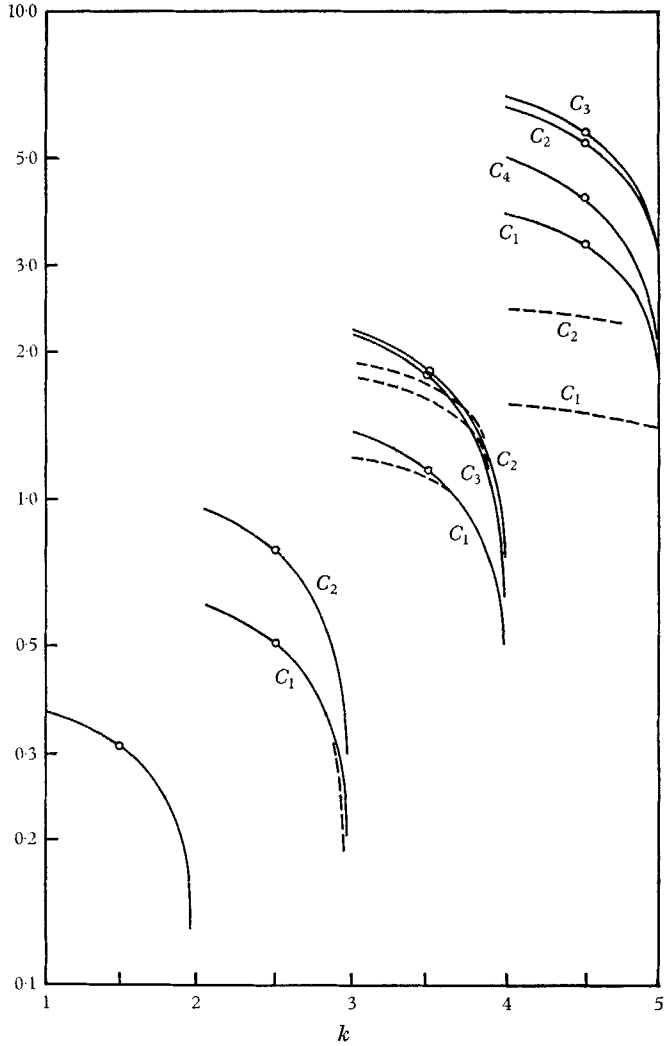

FIGURE 1. The lee-wave amplitude parameter C_n for a thin barrier of height $\frac{1}{4}\pi$. The solid lines are from the numerical solution, the circles from Drazin & Moore and the dashed lines from Miles's variational approximation. For $k > 4$ the variational approximation is inaccurate and only C_1 and C_2 are shown.

0·10 g/cm^3 and the deviation from a linear density distribution was less than five per cent of this difference except within an approximately 1 cm diffusion layer at the bottom of the tank. As a means of visualizing the flow as well as determining the density structure drops of several carbon tetrachloride/kerosene solutions which had been coloured with different oil-soluble dyes were sprayed into the

fluid and allowed to settle to the level where they were neutrally buoyant. Cylindrical obstacles of various shapes were fastened to the bottom of a floating platform 20 cm long which was towed down the tank at a uniform speed. The Reynolds number, based on barrier height, typically varied from 800 for the large values of k^2 to 3000 for runs at small k^2.

A permanent record of the flow was provided by colour photographs which were obtained using an exposure time short enough to 'freeze' the motion. From these transparencies it was possible to determine accurately the position of the layers of neutrally buoyant droplets which, since the flows were approximately

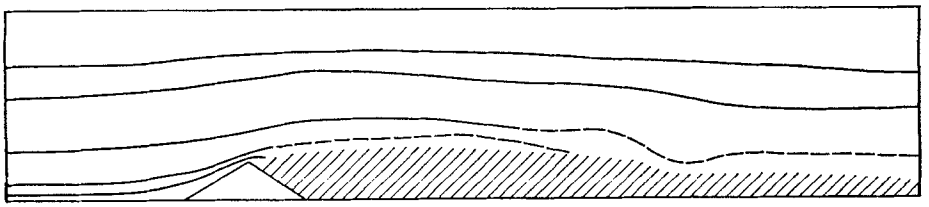

FIGURE 2. Observed flow over triangular obstacle for $k = 0{\cdot}65$.

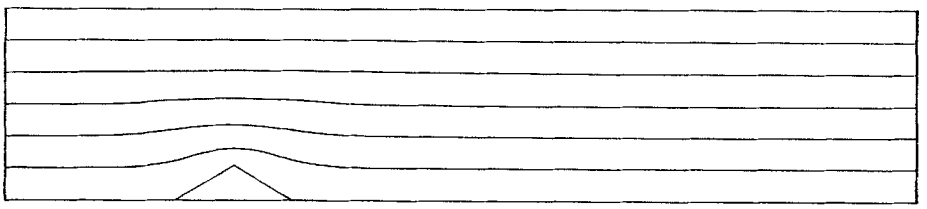

FIGURE 3. Calculated flow over triangular obstacle for $k = 0{\cdot}65$.

steady, correspond to the streamline positions calculated in the theoretical development. In addition, regions of highly turbulent motion were apparent not only from the confused nature of the droplet distribution but also from small-scale variations in light intensity caused by the large gradients of refractive index associated with turbulent mixing.

Unfortunately, from black-and-white reproductions of the colour photographs it is not possible to distinguish droplets from different layers and therefore such reproductions are unsuitable for illustrating the flow. Consequently, for the purposes of this paper, the colour transparencies have been used to construct the line drawings shown in figures 2, 4, 6, 8, 10, 12 and 13. In these drawings a solid line represents the position of a layer of marker drops which were not seriously perturbed by small-scale turbulent motions, and a dashed line indicates the central position of a line of drops which had been dispersed by small-scale motions but not to the point that it had lost its identity as a line. The shaded areas are regions of the flow which were so turbulent that marker particles were uniformly distributed throughout. The nature of the flow implied by the line drawings can be seen by comparing figure 4(*a*) with figure 4(*b*), plate 1, which is a reproduction of the transparency from which the drawing was constructed. In the experiment the obstacle was, of course, placed at the top of the tank, but in the

illustrations this configuration has been inverted to conform with the more usual geometry of flow over a barrier.

Figure 2 illustrates an example of supercritical flow ($k = 0{\cdot}65$) over a triangular barrier of dimensionless height $\frac{3}{16}\pi$ and width $\frac{5}{8}\pi$. For comparison, figure 3 is a plot of streamline positions calculated for the same conditions using the numerical method outlined in the previous section. The considerable influence of boundary-layer separation and the formation of a turbulent wake, both unaccounted for in the theory, is indicated by the fact that the streamlines reach maximum elevation some distance behind the obstacle and that the observed streamline displacements are considerably larger than predicted. This same effect occurs in unstratified flow over bluff bodies, and the only obvious effect of stratification is the suppression of the turbulent wake downstream of the body.

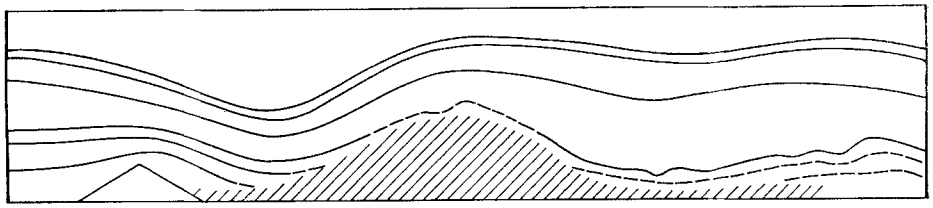

FIGURE 4(*a*). Observed flow over triangular obstacle for $k = 1{\cdot}55$.

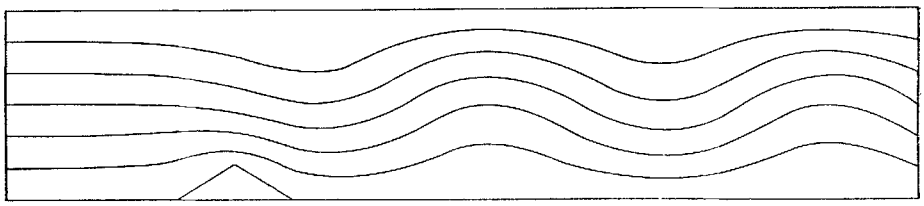

FIGURE 5. Calculated flow over triangular obstacle for $k = 1{\cdot}55$.

Figures 4 to 7 concern flows for the range $1 < k < 2$ in which a single mode of lee wave is excited. In figures 4 and 5, which represent observed and predicted flows over the triangular obstacle for $k = 1{\cdot}55$, the effects of boundary-layer separation and turbulence are again evident. The point of separation is much further downstream than in the supercritical case and the flow presses down over the rear face of the obstacle even more completely than the theory would predict. However, under the first wave trough the boundary layer separates, causing the flow under the first wave crest to become highly turbulent. Typically, in all the experiments performed, the wave amplitudes downstream were smaller than predicted. It is likely that in this case part of the discrepancy is due to the transient nature of the experiments, but results presented in the next section indicate that not all the discrepancy can be ascribed to this and therefore it seems probable that the turbulent motions extract some of the energy which would otherwise go into wave motion. This effect is much more evident in the examples of flow at higher values of k which are discussed below.

Figures 6 and 7 depict flow over a thin vertical barrier of dimensionless height $\frac{1}{4}\pi$ for $k = 1{\cdot}50$. Here again the wake immediately behind the obstacle is compressed by the first wave trough, which presses down even farther than predicted, and the region under the first crest is highly turbulent. Above the first trough there is an isolated region of turbulence which, in the experiment itself, was observed to

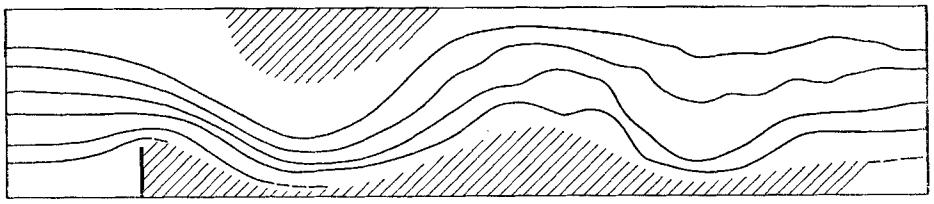

FIGURE 6. Observed flow over thin barrier for $k = 1{\cdot}50$.

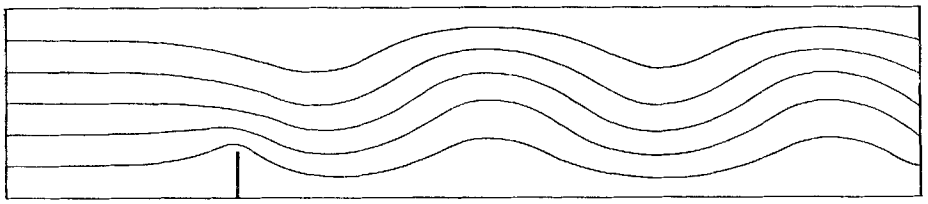

FIGURE 7. Calculated flow over thin barrier for $k = 1{\cdot}50$.

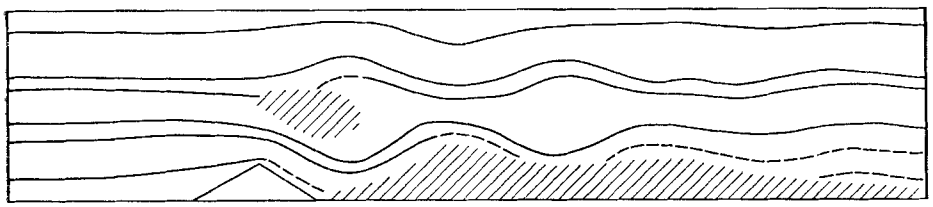

FIGURE 8. Observed flow over triangular obstacle for $k = 2{\cdot}70$.

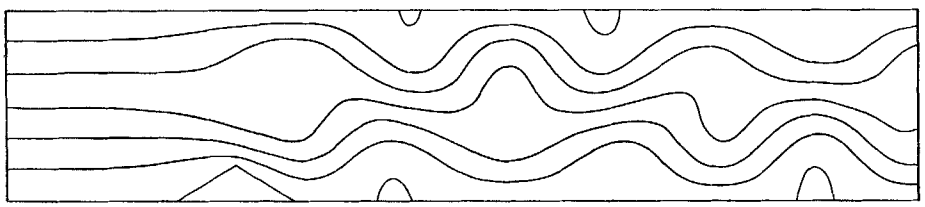

FIGURE 9. Calculated flow over triangular obstacle for $k = 2{\cdot}70$.

move along with the obstacle as a body of slowly mixing fluid. The predicted flow pattern contains no hint of this bubble. As in the flow over the triangular barrier, the observed wavelength is consistent with the theory but the position of the first wave crest is displaced well downstream from its predicted position.

Figures 8–11 deal with flows which are subcritical with respect to two modes of lee wave. Here, for the first time, the predicted flows contain regions of closed streamline flow which, as has been mentioned earlier, are not consistent with the

assumptions upon which the theoretical model is based. The prediction of Long (1955) and Miles (1968*a*) that such closed streamline regions are likely to be unstable seems to be substantiated by the occurrence of turbulent patches in the centre of the rotor regions. As in the two previous examples, the streamlines in both the observed flows press down behind the obstacle and then appear to separate, causing the flow to become highly turbulent. The flow over the triangular obstacle is not seriously affected by this turbulence and, as in the cases discussed earlier, the wavelength, amplitude and horizontal position of the dominant

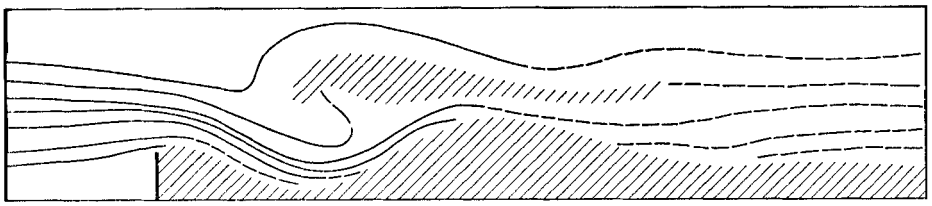

FIGURE 10. Observed flow over thin barrier for $k = 2{\cdot}25$.

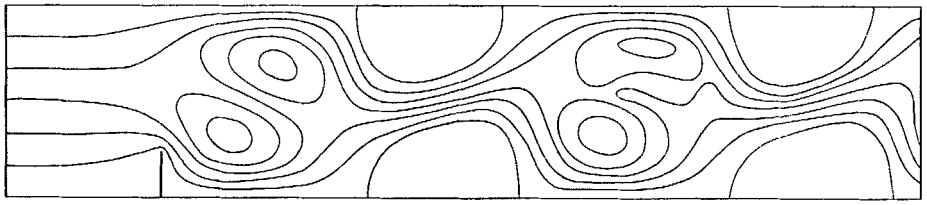

FIGURE 11. Calculated flow over thin barrier for $k = 2{\cdot}25$.

lee wave are in moderate agreement with theory. The flow over the thin barrier, on the other hand, bears very little resemblance to the predicted flow. The flow immediately behind the obstacle is apparently laminar but, as in the other examples discussed, the boundary layer seems to separate as soon as the flow along the boundary begins to decelerate; in this case the resulting turbulence completely destroys the lee-wave structure. Presumably the distinction between the two obstacles lies in the fact that, judging from the amplitudes of the predicted lee waves, the thin barrier constitutes a much greater disturbance to the flow and therefore produces a more violently turbulent wake.

For values of k greater than 3, the flow takes on a character quite unlike that predicted by Long's model. The flows depicted in figures 12 and 13 are typical of this régime and may be contrasted with the formal solutions presented by Drazin & Moore (1967) for large k. While the figures depict flows in the range $3 < k < 4$, the flows observed in the range $4 < k < 5$ were virtually identical. Instead of the very complex lee-wave patterns predicted by the theoretical model, it can be seen that those streamlines which originate at elevations greater than the obstacle height are practically undisturbed. On the other hand, the lower streamlines are laminar as they flow up and over the obstacle, and then become highly turbulent and break down to form a well-mixed wake of approximately the same height as the obstacle.

One final point of interest concerning the flow visualization experiments is the question of the nature of the flow upstream of the obstacle. It may be recalled that the theoretical model is based on the assumptions that the velocity is everywhere continuous and that there are no waves upstream of the obstacle. As a consequence of these assumptions the model predicts that all disturbances to the parallel flow die out exponentially upstream of the obstacle. But these assumptions have been subject to considerable controversy beginning with Long's (1955) observation of a region of jet flow upstream of the obstacle.

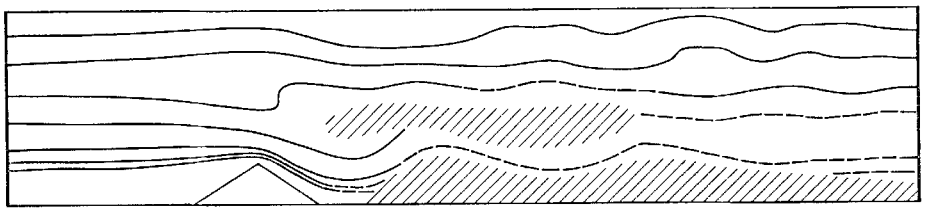

FIGURE 12. Observed flow over triangular obstacle for $k = 3{\cdot}40$.

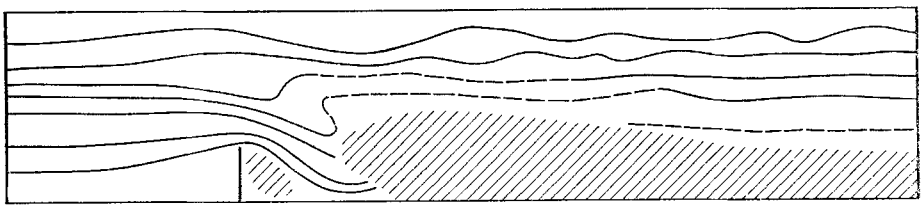

FIGURE 13. Observed flow over thin barrier for $k = 3{\cdot}60$.

Trustrum (1964) investigated the initial value problem corresponding to Long's model and suggested that the final state may involve waves upstream while Bretherton (1967) solved the initial value problem for the limit $k \to \infty$ and found that ahead of the obstacle there is a 'blocked' region of stagnant fluid which is separated from the main flow by a thin shear layer. (Kao (1965) assumed that such blocked regions exist and calculated flows over barriers using an *ad hoc* modification of Long's model.) The phenomenon of blocking has been investigated experimentally by Maxworthy (1968) for the analogous situation in a sphere in a rotating fluid.

In no case investigated here were any waves observed upstream of the obstacle and observation of vertical dye streaks positioned in front of the barrier disclosed neither the jets seen by Long nor any obvious region of blocked flow. There are quite significant discrepancies between the theoretical and observed position of the streamlines upstream of the barrier but it is not possible to determine how much of this is due to blocking and how much is due to the upstream influence of the discrepancies found in the wake. It is, however, evident from the examples presented, as well as from additional experiments in the range $4 < k < 5$, that the effects of upstream blocking, if it occurs, are insignificant compared with the other differences between theory and experiment.

Drag and wave drag

In addition to the flow visualization experiments described in the previous section, a series of experiments were performed to determine how the drag on an obstacle is influenced by stratification. In order to accomplish this it was felt desirable to measure both the total drag on the obstacle and the amplitudes of the various lee-wave modes, from which the wave drag could be computed. According to Long's laminar inviscid flow model the total drag and the wave drag are equal but, owing to the discrepancies between this theory and the experimental observations, it would be unreasonable to presume that this would be the case.

Unfortunately it was impossible to make accurate total drag measurements on obstacles which were contiguous with either of the horizontal boundaries of the fluid. Attempts to tow the barrier along the lower boundary were abandoned because of the errors introduced by frictional drag on the bottom while attempts to measure the drag on an obstacle towed along the free surface were overcome by surface tension forces resulting from the fact that the obstacle compressed a surfactant-contaminated surface film as it swept down the tank. Consequently the obstacle, a thin barrier of dimensionless height $\frac{1}{4}\pi$, was suspended on thin wire supports below a floating platform consisting of two narrow floats which were aligned parallel to the direction of motion. The top of the barrier was $\frac{1}{4}\pi$ below the free surface. The entire assembly was attached to a pendulum balance mounted on a second floating platform which was then towed ahead of the barrier assembly at a uniform speed. During the course of such a run the drag on the barrier assembly was recorded and simultaneously photographs of the type described in the previous section were taken to record the position of several different layers of marker particles.

From (6) in the second section it is seen that far downstream of the barrier the lee-wave structure becomes dominant and

$$\delta \sim \sum_{n=1}^{K} \alpha_n^{-1} C_n \sin ny \sin \alpha_n (x + \theta_n).$$

As Miles (1968*a*) has shown, this leads to a drag on the barrier, D, which may be characterized by the wave drag doefficient

$$C_{DW} = \left(\frac{1}{2} q \frac{H}{\pi} d\right)^{-1} D = \frac{\pi}{2d} \sum_{n=1}^{K} C_n^2, \tag{7}$$

where d is the dimensionless vertical chord of the barrier. From this relation the wave drag coefficient can be calculated once the amplitudes of the various lee-wave modes are known. In order to estimate the amplitudes, C_n, the values of $\delta(x, y)$ at each of several horizontal stations, x_i, were fitted in a least square error sense to the form

$$\delta(x, y) = \sum_{n=1}^{N} A_n (x_i) \sin ny,$$

where N was either K or $K+1$. The resulting values of A_n for $n \leqslant K$ were insensitive to the choice of N and A_{K+1} was always small; if any periodicity was evident, the wavelength was that of one of the lower modes.

While the primary purpose of this modal decomposition was the determination of the lee-wave amplitudes, the curves $A_n(x)$ contain some interesting information concerning the transient nature of the experiments. This can be seen in figure 14, in which the curves labelled (*a*) and (*b*) are $A_1(x)$ for $k = 1{\cdot}35$ and $k = 1{\cdot}50$ respectively and (*c*) and (*d*) are $A_1(x)$ and $A_2(x)$ respectively for $k = 2{\cdot}20$. With the exception of (*c*), these curves indicate a decrease of both

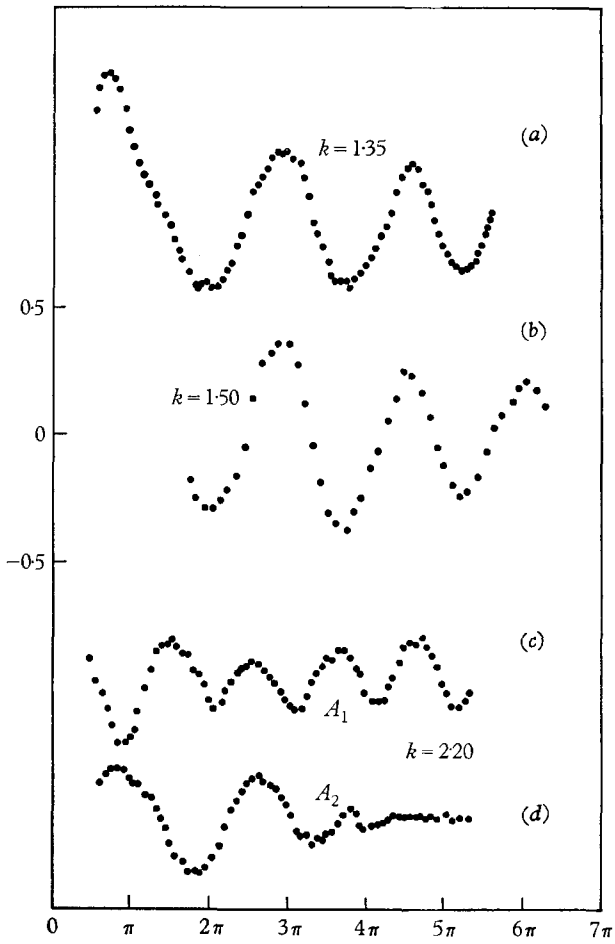

FIGURE 14. The lee-wave amplitude parameter $A_n(x)$ used in determining wave drag. The vertical scale is the same for each curve.

amplitude and wavelength with increasing distance behind the barrier. Because the group velocity of these waves decreases with decreasing wavelength, it is reasonable to ascribe this effect to the dispersion of the transient lee waves. Presumably the slower-moving short-wavelength waves were falling behind the barrier as the flow approached the steady state which involves only periodic lee-wave components. This situation is similar to the development of a surface wave behind a moving disturbance which has been studied by Wurtele (1955) and, indeed, the curves in figure 14 bear a strong resemblance to the development he

predicted. Long (1955) also found that lee-wave amplitudes decreased downstream; since, in terms of wavelength, his channel length is comparable to that used here it is likely that dispersive effects were responsible for some of this decrease.

The results of the drag experiments are contained in figure 15, where the total drag coefficient, C_{DT}, measured for the range $0 < k < 4$ is plotted along with measured wave drag coefficients for the range $1 < k < 3$. In those cases where the flow was far from the steady state the estimates of lee-wave amplitude are subject

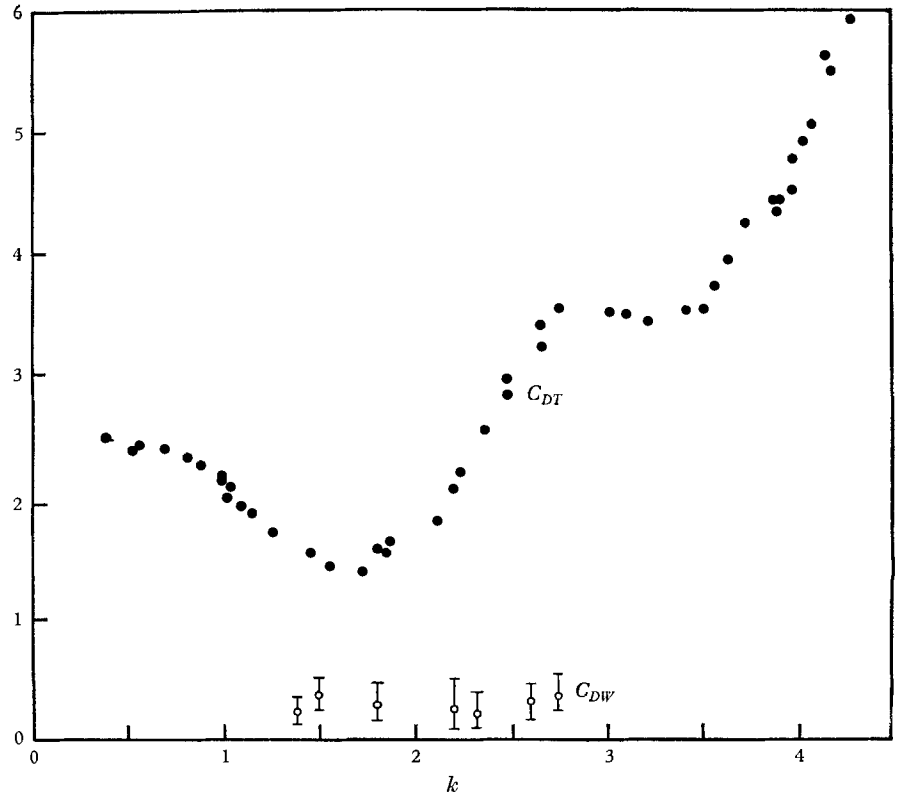

FIGURE 15. Measured values of total drag coefficient, C_{DT}, and wave drag coefficient, C_{DW}, for a thin barrier of height $\frac{1}{4}\pi$ placed with one edge at a height of $\frac{1}{2}\pi$.

to considerable uncertainty, but in most cases (curve (*a*) being an exceptional case) the amplitudes C_n could be determined to within 25 %. The wave-drag coefficients calculated from (7) may, therefore, be in error by a factor of 1·5. As in the cases discussed in the previous section, for $k > 3$ the flow in the wake of the barrier was so turbulent that the lee-wave modes could not be identified. Total drag measurements for $k > 4$ were abandoned because the drag no longer reached a steady value during the course of an experiment, apparently because the operation of towing the barrier became unstable when the drag became a decreasing function of speed.

The data in figure 15 serve to point out certain interesting facts concerning the drag associated with stratified flow. First, the drag on an object may be

substantially increased or reduced as a result of stratification. Secondly, the drag associated with lee-wave generation is not, for the thin barrier at least, the dominant effect of stratification. Thirdly, as can be seen by the behaviour of the total drag coefficient in the neighbourhood of $k = 4$, stratification can lead to the situation where the total drag on an obstacle increases as the speed of the obstacle decreases. Finally, the absence of any organized wave structure for $k > 3$ tends to corroborate the observation made in the previous section that the complex lee-wave patterns found in solutions of the theoretical model for large k are apparently unstable and do not occur in real flows.

Unfortunately it is not possible to make a proper comparison between measured wave drag and that predicted by Long's model because, as mentioned in connexion with the theoretical model, without further hypothesis the model can be applied only to obstacles which are contiguous to one of the horizontal boundaries. As in the theory of external potential flows, some additional constraint must be imposed to determine the position of the stagnation points and hence to obtain an unambiguous solution. However, for an infinitely thin barrier it seems quite reasonable to require that the lift on the obstacle be zero. When this constraint, which, it can be shown, is equivalent to requiring that the circulation computed along the obstacle surface vanish, is included in the specification of the theoretical model the problem becomes determinate and the techniques described earlier can then be used to calculate predicted flow patterns and drag coefficients. Comparison of the predicted and observed positions of the front stagnation point indicates that the zero-lift hypothesis is reasonable, although the experimental precision is insufficient to detect small discrepancies. The predicted drag coefficients are much smaller than for a barrier of the same height which is adjacent to a boundary. In the range $1 < k < 2$ the predicted value of C_{DW} falls between 0·04 and 0·10, which is significantly smaller than the observed wave drag coefficient, while for $2 < k < 3$ the observed coefficients are in reasonable agreement with the predicted values, which fall between 0·3 and 0·5.

Conclusion

This study was originally motivated by the theoretical studies of Drazin & Moore (1967) and Miles (1968*a*) which were based on Long's equation for the motion of a stratified fluid. These investigations, which were the first to calculate exactly the flow over obstacles of prescribed shape, predicted that the excitation of lee waves could lead to extremely large drags. However, as Miles pointed out, these predictions are subject to two serious objections: namely those solutions which are associated with large drags are not consistent with the derivation of Long's equation and, even if they are interpreted as legitimate steady-state flows, these solutions probably represent unstable motions.

Measurements of wave drag and total drag demonstrated that, while the influence of stratification on drag is considerable, this effect is due, in large part, to phenomena which are not described by Long's equation. This discovery led, in turn, to an investigation of the discrepancies between theoretically predicted flows and those observed experimentally. Towards this end, a simple method of

solving Long's model for arbitrary prescribed obstacles was devised and the resulting flow patterns were compared with experiment.

On the surface, the experimental procedure adopted here appears to include two obvious improvements over that used by Long (1955). First, the same obstacle was used in the theoretical calculations and in the corresponding experiment. Secondly, the stratification was much more carefully controlled than in the earlier experiments and, in contrast to the method employed by Long, a smooth variation of density as well as a nearly constant density gradient was assured by the manner in which the tow tank was filled. The first improvement is of little consequence since the discrepancy between experiment and theory invariably overshadows the slight difference in the method of calculating the theoretical solution. The fact that the fluid is strongly stratified even near the boundary supporting the obstacle may, however, account for some of the differences between Long's observations and those made here, particularly in reference to upstream influence.

As long as only a few lee-wave modes have been excited the observed flow is qualitatively similar to that predicted. The most obvious discrepancies are due to turbulence associated with boundary-layer separation and to isolated patches of turbulence which seem to occur where the theory would predict almost vertical, or even closed, streamlines. It is interesting to note that the point of boundary-layer separation is strongly influenced by the lee-wave structure and that typically the major source of turbulence seems to be boundary-layer separation under the first lee-wave trough. This separation is apparently caused by the adverse pressure gradient encountered by the boundary layer after it passes through the low-pressure region under the first trough; an adverse pressure gradient may also account for the large turbulent bubble found on the boundary opposite the obstacle in figure 6. The internal patches of turbulence may be due either to a statically unstable density configuration or to excessive shear. Both turbulence production mechanisms are associated with steep lee waves. The experiments indicate that the lee-wave amplitudes decrease downstream; Long observed this and attributed it to turbulence. The experiments of the fourth section indicate that, in both experimental programmes, this is partly the result of dispersive effects; it should be noted in this context that curve (*c*) in figure 14 shows little spatial decay although the small-scale distortions are surely the result of turbulence.

It is not until the flow becomes subcritical with respect to several lee-wave modes that the predicted drag coefficients become anomalously large and it is for this condition that the theoretical model no longer provides even a qualitative picture of real flows. When the parameter k becomes large, turbulence becomes dominant and the flow in the wake of the obstacle may be described as an internal hydraulic jump. The flow remains laminar as it passes over the obstacle and forms an intense jet immediately downstream. Then this jet suddenly separates from the horizontal boundary behind the obstacle and erupts into a violently turbulent wake of approximately the same height as the obstacle. Those streamlines which originate at heights greater than the obstacle are not greatly disturbed by the barrier and in no part of the wake is there any evidence of organized wave

motion. This distinctive flow régime was apparently not observed by Long probably because he had intentionally restricted his study to conditions for which the theoretically predicted flow appeared to be stable. This type of flow is, however, deserving of study and may be of considerable importance on a meteorological scale (figure 21 of Lighthill's (1967) article on waves may be an example of this régime). The fact that the upstream jets observed by Long could not be detected remains unexplained.

In conclusion, it seems fair to say that solutions of Long's model provide a qualitative picture of real stratified flows only for a limited range of conditions. The anomalous drag coefficients and complex lee-wave wakes predicted by the application of the theory outside this range of conditions are spurious.

This work was supported by the National Science Foundation under Grant GA-849.

The author is indebted to Prof. J. W. Miles and Dr H. E. Huppert for many useful discussions concerning the subject of this paper.

REFERENCES

Bretherton, F. 1967 The time-dependent motion due to a cylinder moving in an unbounded rotating or stratified fluid. *J. Fluid Mech.* **28**, 545.

Drazin, P. G. & Moore, D. W. 1967 Steady two-dimensional flow of a fluid of variable density over an obstacle. *J. Fluid Mech.* **28**, 353.

Jolley, L. B. W. 1961 *Summation of Series.* New York: Dover.

Kao, T. 1965 The phenomenon of blocking in stratified flows. *J. Geophys. Res.* **70**, 815.

Lighthill, M. J. 1967 Waves in fluids. *Commun. Pure Appl. Math.* **20**, 267.

Long, R. R. 1953 Some aspects of the flow of stratified fluids; I. A theoretical investigation. *Tellus*, **5**, 42.

Long, R. R. 1955 Some aspects of the flow of stratified fluids; III. Continuous density gradients. *Tellus*, **7**, 341.

Maxworthy, T. 1968 The observed motion of a sphere through a short, rotating cylinder of fluid. *J. Fluid Mech.* **31**, 643.

Miles, J. W. 1968*a* Lee waves in a stratified flow. Part 1. Thin barrier. *J. Fluid Mech.* **32**, 549.

Miles, J. W. 1968*b* Lee waves in a stratified flow. Part 2. Semi-circular obstacle. *J. Fluid Mech.* **33**, 803.

Trustrum, K. 1964 Rotating and stratified fluid flow. *J. Fluid Mech.* **19**, 415.

Wurtele, M. G. 1955 The transient development of lee waves. *J. Marine Res.* **14**, 1.

Yih, C. 1960 Exact solutions for steady two-dimensional flow of a stratified fluid. *J. Fluid Mech.* **9**, 161.

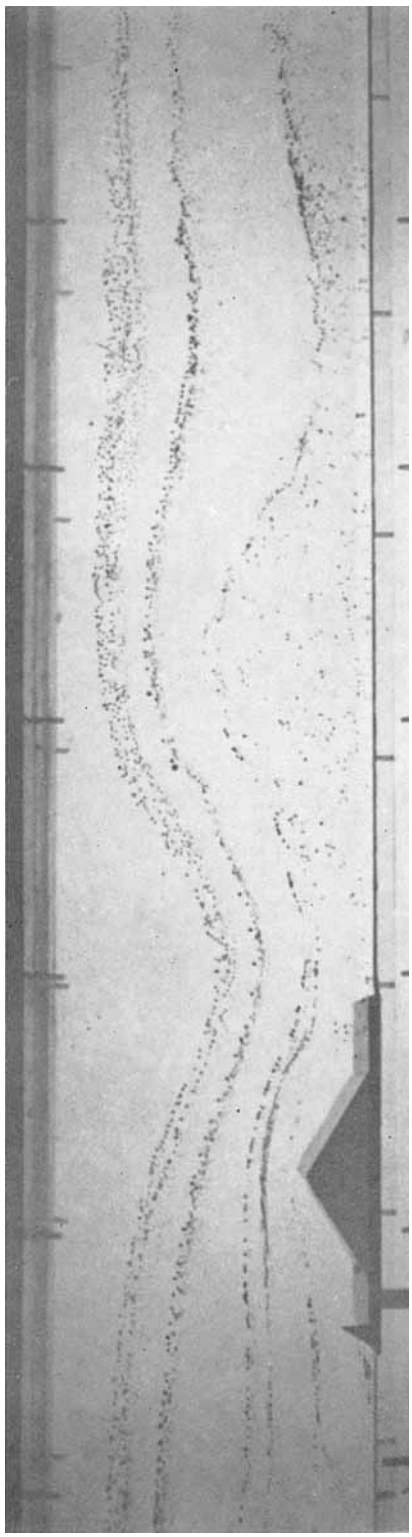

FIGURE 4(*b*). Reproduction of the transparency from which figure 4(*a*) was drawn.